

Research Paper

Cite this article: López-Jiménez A, González-García MT, Andrade-Gómez L, García-Varela M (2023). Phylogenetic analyses based on molecular and morphological data reveal a new species of *Strigea* Abildgaard, 1790 (Digenea: Strigeidae) and taxonomic changes in strigeids infecting Neotropical birds of prey. *Journal of Helminthology* **97**, e35, 1–15. <https://doi.org/10.1017/S0022149X23000196>

Received: 2 March 2023

Revised: 21 March 2023

Accepted: 22 March 2023





Keywords:

Strigeidae; phylogeny; *Strigea*; molecular markers; taxonomy

Author for correspondence:

A. López-Jiménez; Email: aleloji@ciencias.unam.mx

Phylogenetic analyses based on molecular and morphological data reveal a new species of *Strigea* Abildgaard, 1790 (Digenea: Strigeidae) and taxonomic changes in strigeids infecting Neotropical birds of prey

A. López-Jiménez^{1,2} , M.T. González-García^{1,2} , L. Andrade-Gómez³ 
and M. García-Varela¹ 

¹Departamento de Zoología, Instituto de Biología, Universidad Nacional Autónoma de México (UNAM), Mexico City, Mexico; ²Posgrado en Ciencias Biológicas, Unidad de Posgrado, CDMX, Mexico and ³Escuela Nacional de Estudios Superiores, Unidad Mérida, Yucatán, Mexico

Abstract

Members of the genus *Strigea* Abildgaard, 1790 are endoparasites of birds distributed worldwide. Adults of an undescribed species of the genus *Strigea* were collected from the intestines of two hawk species (*Rupornis magnirostris* and *Accipiter cooperii*). Other species identified as *Parastrigea macrobursa* that were described in Argentina were also recovered from two hawk species (*Buteogallus urubitinga* and *Buteogallus anthracinus*) in three localities along the coasts of Mexico. Specimens of the two species were sequenced for three molecular markers, the internal transcribed spacers locus (ITS1–5.8S rDNA–ITS2) and the domains D1–D3 from the large subunit from nuclear ribosomal DNA and the cytochrome *c* oxidase subunit 1 from mitochondrial DNA. The newly sequenced specimens were aligned with other strigeids sequences downloaded from GenBank. Maximum likelihood and Bayesian analyses inferred with each molecular marker revealed that our specimens of *Strigea* sp. formed an independent lineage, which is recognized herein as a new species, *Strigea magnirostris* n. sp., representing the first species in Mexico and the 16th in the Neotropical region. Morphologically, the new species is distinguished from other congeneric species from the Americas by having an oral sucker with several papillae around it, well-developed pseudosuckers (118–248 µm), a tegument covered with tiny spines, a larger cone genital (193–361 × 296–637) and a larger copulatory bursa (247–531 × 468–784). Our phylogenetic analyses revealed that *P. macrobursa* is not closely related to other members of the genus *Parastrigea* and is nested within *Strigea*, suggesting that *P. macrobursa* should be transferred to *Strigea* to form *Strigea macrobursa* n. comb., expanding its distribution range from Mexico to Argentina. Finally, the analyses also revealed that the taxonomy and systematics of *Strigea* should be re-evaluated, combining morphological and molecular characteristics.

Introduction

The cosmopolitan family Strigeidae Railliet, 1919 currently contains 13 genera with approximately 110 nominal species distributed worldwide (Niewiadowska, 2002). The type genus *Strigea* was established by Abildgaard, 1790 to accommodate species that have vitellarium uniformly distributed over both parts of the body and the presence of a pharynx (Dubois, 1968; Niewiadowska, 2002). Among strigeids, *Strigea* is considered the most diverse genus within the family, with approximately 47 nominal species associated mainly with strigiform, accipitriform, falconiform, ciconiiform, caprimulgiform, cariamiform, passeriform, gruiform, trogoniform and anseriform birds (Dubois, 1968; Drago *et al.*, 2014). Information on the life cycle of most species of *Strigea* is scarce, but it is thought to involve four hosts. Adult worms live and reproduce sexually in the digestive tracts of birds that serve as definitive hosts. Eggs are expelled into the environment with the faeces of the host. After the ingestion of the eggs by a planorbid snail, which serves as the first intermediate host, the parasites develop into cercariae. The cercariae emerge and swim to find and penetrate the second intermediate host (amphibians), where they develop into mesocercariae and in some cases it may cause severe morphological anomalies as the polydactyly (Sinsch *et al.*, 2019; Svinin *et al.*, 2020, 2023). The amphibian with the mesocercaria is ingested by the third intermediate host (an amphibian, reptile, bird, or small mammal) and then the parasite develops into an encysted, tetracotyle-type metacercaria. Finally, these amphibians, reptiles, birds and mammals

© The Author(s), 2023. Published by Cambridge University Press. This is an Open Access article, distributed under the terms of the Creative Commons Attribution licence (<http://creativecommons.org/licenses/by/4.0/>), which permits unrestricted re-use, distribution and reproduction, provided the original article is properly cited.



are some of the principal food resources of prey birds, in which the life cycle is completed (Pearson, 1959, 1972; Odening, 1967).

To date, *Strigea* contains 47 described species, nine of which are distributed in Asia, nine in Africa, five in Oceania and three in Europe (Dubois, 1968, 1988; Dubois & Beverley-Burton, 1971). In the Americas, 21 species have been described, of which six are in North America (*Strigea infundibuliformis* Dubois, 1934; *Strigea macroconophora* Dubois and Rausch, 1950; *Strigea elegans* Chandler and Rausch, 1947; *Strigea sphaerula macrosicya* Dubois and Rausch, 1950; *Strigea gruis* Dubois and Rausch, 1964 and *Strigea macropharynx* Dubois and Rausch, 1965); and 15 species in South America (*Strigea caryophylla* (Diesing, 1850) Mathias, 1925; *Strigea elliptica* (Brandes, 1888) Szidat, 1928; *Strigea bulbosa* (Brandes, 1888) Szidat, 1928; *Strigea nugax* Szidat, 1928; *Strigea vaginata* (Brandes, 1888) Szidat, 1928; *Strigea falconis brasiliiana* Szidat, 1929; *Strigea caluri* Dubois, 1962; *Strigea sphaerocephala* (Westrumb, 1823) Dubois, 1937; *Strigea microbursa* Pearson and Dubois, 1985; *Strigea magniova* Dubois, 1988; *Strigea arcuata* Dubois, 1988; *Strigea meridionalis* Lunaschi and Drago, 2009; *Strigea inflecta* Lunaschi and Drago, 2012; *Strigea orbiculata* Lunaschi and Drago, 2013 and *Strigea proteolytica* Drago, Lunaschi and Draghi, 2014) (Dubois, 1968; Lunaschi & Drago, 2006, 2009, 2012, 2013; Drago *et al.*, 2014). The morphological identification of *Strigea* spp. is complex and problematic due to their small size and the difficulty in observing internal and external structures used for taxonomy and differentiation among species (Lunaschi & Drago, 2006, 2009, 2012, 2013; Drago *et al.*, 2014). Additionally, molecular data are scarce and only a few sequences of *Strigea* are currently available (Hernández-Mena *et al.*, 2017; Heneberg *et al.*, 2018; Svinin *et al.*, 2020). In Mexico, the metacercaria of *Strigea* was recorded for the first time by Vidal-Martínez (1995) in two cichlid fish species in south-eastern Mexico (Pérez-Ponce de León *et al.*, 2007). However, the specimens were not deposited, and therefore, the records could not be verified. Hernández-Mena *et al.* (2017) recorded an adult of *Strigea* sp. in crested caracara (*Caracara cheriway* Jacquin) in Presa La Angostura, Chiapas, Mexico. Recently, strigeids in Mexico have started to receive attention and much effort has been made to incorporate morphological and molecular characteristics to describe and delineate the biodiversity of this group of parasites (Hernández-Mena *et al.*, 2014, 2017; López-Jiménez *et al.*, 2021, 2022).

In the current study, adult specimens of the genus *Strigea* were collected from the intestine of roadside hawk (*Rupornis magnirostris* Gmelin) and Cooper's hawk (*Accipiter cooperii* Bonaparte) in six localities from the Neotropical region of Mexico. After a careful morphological examination, the specimens were determined to correspond to an undescribed species of the genus *Strigea*. In addition, other strigeids collected from the intestine of the great black hawk (*Buteogallus urubitinga* Gmelin) and common black hawk (*Buteogallus anthracinus* Deepe) were identified as *Parastrigea macrobursa* Drago & Lunaschi, 2011, a species previously described in South America.

The objectives of the present research were: (a) to provide a morphological description of the new species; and (b) to test the systematic position of *P. macrobursa* by using sequences of the internal transcribed spacers (ITS1-5.8S rDNA- ITS2) and large subunit (LSU) of the nuclear DNA and of the cytochrome c oxidase subunit I (*cox 1*) gene of the mitochondrial DNA. We

then used the resulting phylogenetic trees as a framework to discuss host-parasite associations and begin to understand the evolutionary history of this group of strigeids.

Materials and methods

Specimen collection

A total of 17 hawks were collected between December 2019 and December 2021 in nine localities from Mexico (fig. 1; table 1). Ten individuals of roadside hawk (*R. magnirostris*), one Cooper's hawk (*A. cooperii*), two individuals of great black hawk (*Buteogallus urubitinga*) and four common black hawks (*B. anthracinus*). Birds were identified following Howell & Webb (1995) and the American Ornithologist' Union (1998) guidelines. Strigeids were removed from the intestines of the birds and examined using a stereomicroscope. Digeneans collected were relaxed in hot distilled water and preserved in 100% ethanol for morphological and molecular analyses.

Morphological analyses

Digeneans preserved in 100% ethanol were stained with Mayer's paracarmine (Merck, Darmstadt, Germany), dehydrated in ethanol series, cleared in methyl salicylate and mounted in Canada balsam for morphological analysis. Specimens were examined using a compound microscope equipped with a bright field Leica DM 1000 light emitting diode microscope (Leica, Wetzlar, Germany). Measurements were taken using Leica Application Suite microscope software (Leica Microsystems GmbH, Wetzlar, Germany) and are given in micrometres and presented with the range followed by the mean in parentheses. Some specimens were dehydrated with an ethanol series, critical point dried, sputter coated with gold and examined with a Hitachi Stereoscan Model S-2469N scanning electron microscope operating at 15 kV. Voucher specimens from the present study were deposited in the Colección Nacional de Helmintos (CNHE) from Instituto de Biología, Universidad Nacional Autónoma de México (UNAM), Mexico City.

DNA isolation, amplification and sequencing

Strigeids preserved in 100% ethanol were placed individually in tubes and digested overnight at 56°C in a solution containing 20 mM sodium chloride, 10 mM Tris-hydrochloride (pH = 7.6), 100 mM ethylenedinitrilotetraacetic acid disodium salt dihydrate (pH = 8.0), 1% Sarkosyl and 0.1 mg/ml proteinase K. Following digestion, DNA was extracted from the supernatant using the DNAzol reagent (Molecular Research Center, Cincinnati, Ohio). The internal transcribed spacers (ITS1-5.8S rDNA- ITS2) of the nuclear ribosomal DNA were amplified using the forward primer BD1 5'-GTCGTAACAAGGTTTCCGTA- 3' (Bowles & McManus, 1993) and the reverse primer BD2 5'-ATCTAG ACCGGACTAGGCTGTG-3' (Bowles *et al.*, 1995). The partial fragments of domains D1-D3 of the large subunit of nuclear ribosomal RNA (LSU) were amplified with the forward primer 391 5'-AGCGGAGGAAAAGAACTAA-3' (Nadler *et al.*, 2000) and the reverse primer 536, 5' -CAGCTATCCTGAGGGAAAC-3' (García-Varela & Nadler, 2005). The complete gene of the cytochrome c oxidase subunit I (*cox 1*; 850 base pairs (bp)) was amplified using the forward primers AphaF, 5'-TAT GATTTTTTTTTTTTTTTRATG-3' and the reverse primer

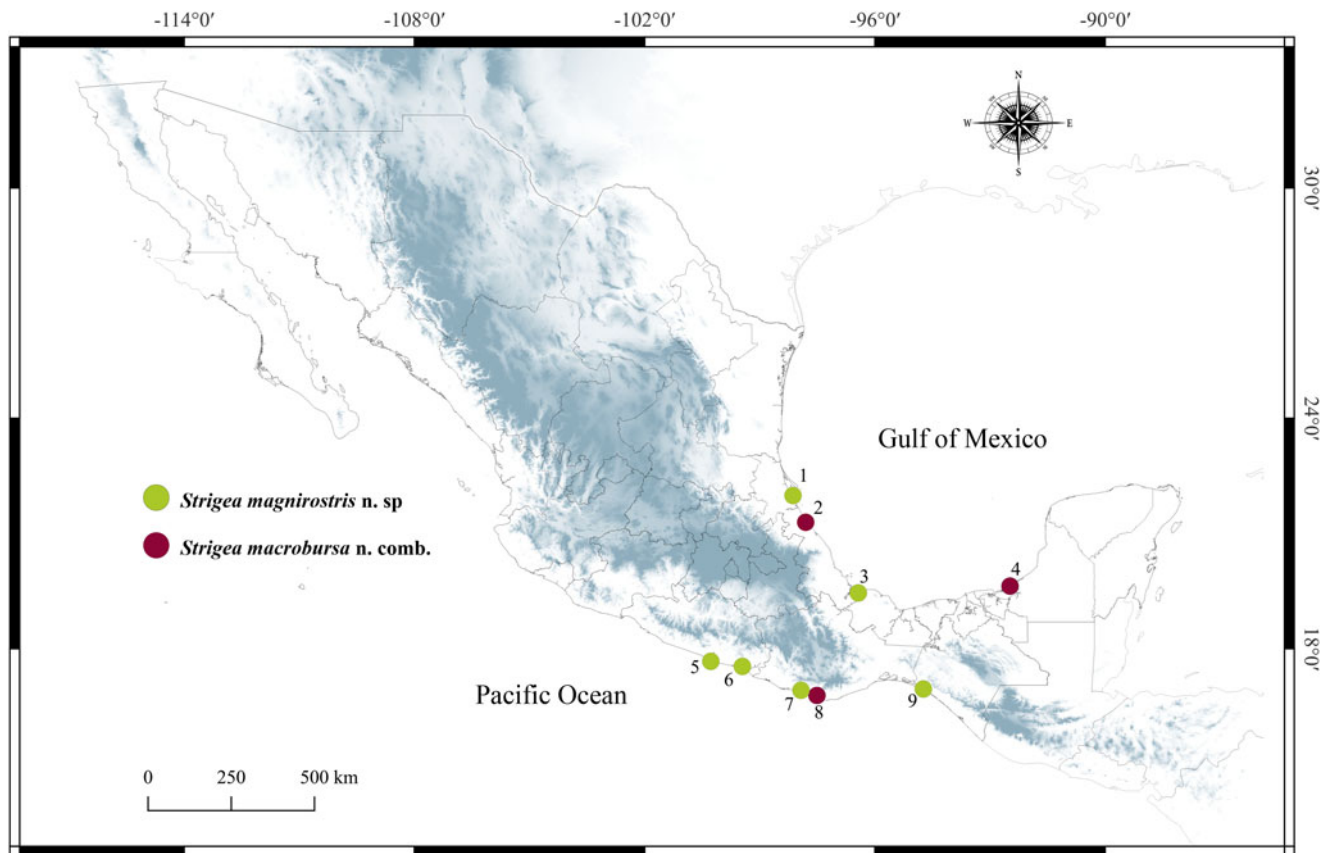


Fig. 1. Map of Mexico showing the sampled sites for the birds. Localities with a circle with colours green and red were positive for the infection with *Strigea magnirostris* n. sp. and *Strigea macrobursa* n. comb., respectively. Localities correspond to those in table 1.

JB4.5'-TAAAGAACATAATGAAATTG3' (Bowles *et al.*, 1992). Polymerase chain reactions (PCRs) were carried out in 25 μ l reactions, consisted of 1 μ l of each primer, 2.5 μ l of 10 \times buffer, 1.5 μ l MgCl₂, 0.5 μ l of dNTP mixture, 0.125 μ l of Platinum Taq DNA polymerase (Invitrogen Corporation, São Paulo, Brazil) and 2 μ l of genomic DNA. PCR cycling parameters for amplifications consisted of denaturation at 94°C for 1 min, 35 cycles of 94°C for 1 min, 50°C for 1 min and 72°C for 1 min, followed by a post-amplification incubation at 72°C for 10 min. Sequencing reactions were performed using ABI Big Dye (Applied Biosystems, Boston, Massachusetts) terminator sequencing chemistry and reaction products were separated and detected using an ABI 3730 capillary DNA sequencer. Contigs were assembled and base-calling differences resolved using Codoncode Aligner version 9.0.1 (Codoncode Corporation, Dedham, Massachusetts) and submitted to the GenBank dataset (table 1).

Alignments and phylogenetic analysis

Newly-generated sequences of ITS, LSU and *cox 1* were aligned with other sequences of strigeids available in the GenBank dataset. Sequences of each molecular marker were aligned using the software CLUSTAL_X (Thompson *et al.*, 1997). The best nucleotide substitution model was selected for each molecular marker using jModelTest v2.1.7 (Posada, 2008) and applying the Akaike information criterion. The best nucleotide substitution model for the ITS and LSU dataset were TVM + I + G and for *cox 1* the dataset was TIM3 + I + G. Phylogenetic trees were

reconstructed through maximum likelihood (ML) with the program RAxML v7.0.4 (Silvestro & Michalak, 2012), and Bayesian inference (BI) analyses were inferred with MrBayes 3.2.2 (Ronquist *et al.*, 2012) using the computational resource Cyberinfrastructure for Phylogenetic Research Science Gateway v3.3 (Miller *et al.*, 2010). ML analyses were inferred with the option GTRGAMMAI and 10,000 bootstrap replicates. BI analyses included Markov chain Monte Carlo searches of two simultaneous runs for 10 million generations, sampling every 1000 generations, a heating parameter value of 0.2 and a burn-in of 25%. Trees were drawn and edited using FigTree software v1.4.0 (Rambaut, 2012). Genetic divergences were estimated using *P* uncorrected distances with MEGA v.6 (Tamura *et al.*, 2013).

Results

Molecular characterization and phylogenetic analyses

Nuclear genes

The ITS dataset included 42 sequences with 1042 characters. The phylogenetic analyses performed with ML and BI showed that the genus *Strigea* is monophyletic and is subdivided into two major subclades (fig. 2). The first subclade was formed by 17 isolates of an undescribed species of *Strigea* sp. from the roadside hawk (*R. magnirostris*) and Cooper's hawk (*A. cooperii*) collected from six localities in Mexico. This clade is sister to another subclade formed by eight isolates identified morphologically as *P. macrobursa* recovered from the great black hawk (*Buteogallus urubitinga*) and common black hawk (*B. anthracinus*) from

Table 1. Specimens' information for *Strigea* spp., locality, state, geographical coordinates, host name, number of host examined/infected (prevalence of infection) and GenBank accession number for specimens studied in the current study.

Locality	State	Coordinates	Host	Host infected/ host revised	Species of <i>Strigea</i>	Internal transcribed spacers	Large subunit	Cytochrome c oxidase subunit 1	
1. Tamiahua	Veracruz	21°18'02" N 97°26'56.2" W	<i>Rupornis magnirostris</i>	1/1	<i>S. magnirostris</i> n. sp.	QO647944	QO647911	QO648146	
						QO647941	QO647912	QO648143	
2. Tecolutla	Veracruz	20°33'49.8" N 97°05'57.7" W	<i>Buteogallus urubitinga</i>	1/1	<i>S. macrobursa</i> n. comb.	QO647932	QO647927	QO648131	
						QO647933	QO647928	QO648130	
						QO647936	QO647929	QO648132	
						QO647935	QO647930	QO648133	
3. Tlacotalpan	Veracruz	18°37'04.15" N 95°38'56.10" W	<i>R. magnirostris</i>	2/2	<i>S. magnirostris</i> n. sp.	QO647942	QO647913	QO648142	
						QO647943	QO647909		
						QO647948	QO647914	QO648144	
						QO647940	QO647910	QO648145	
4. Isla Aguada	Campeche	18°48'22.92" N 91°28'03.68" W	<i>B. urubitinga</i>	1/1	<i>S. macrobursa</i> n. comb.	QO647937	QO647923		
						QO647938	QO647924		
						QO647939	QO647925		
								QO648128	
							QO647926	QO648129	
5. Tres Vídas	Guerrero	16°43'59.85" N 99°42'48.99" W	<i>R. magnirostris</i>	1/3	<i>S. magnirostris</i> n. sp.	QO647949	QO647917	QO648135	
						QO647945	QO647915	QO648140	
			<i>Accipiter cooperii</i>	1/1			QO647946		QO648141
							QO647947	QO647916	QO648147
6. Marquelia	Guerrero	16°35'40.88" N 98°50'37.90" W	<i>R. magnirostris</i>	1/1	<i>S. magnirostris</i> n. sp.	QO647950	QO647918	QO648136	
						QO647951	QO647919	QO648137	
						QO647952		QO648138	
7. Villa de Tututepec	Oaxaca	15°56'10.98" N 97°13'38.87" W	<i>R. magnirostris</i>	1/2	<i>S. magnirostris</i> n. sp.	QO647953	QO647920	QO648139	
			<i>B. anthracinus</i>	0/3					
8. Santa María, Cocotepec	Oaxaca	15°48'24.56" N 97°00'49.79" W	<i>B. anthracinus</i>	1/1	<i>S. macrobursa</i> n. comb.	QO647934	QO647931	QO648134	
9. El Zapotal	Chiapas	15°58'20.26" N 93°51'23.04" W	<i>R. magnirostris</i>	1/1	<i>S. magnirostris</i> n. sp.	QO647954	QO647921		
						QO647955	QO647922		
						QO647956		QO648148	
								QO648149	
							QO648150		

The sample number for each locality corresponds with the same number in [Figure 1](#).

three localities in Mexico. All these relationships were supported with well-supported bootstrap values and Bayesian posterior probabilities ([fig. 2](#)). The intraspecific genetic divergence among 17 isolates of *Strigea* sp. was low, ranging from 0 to 0.3%, whereas that for *P. macrobursa* ranged from 0 to 0.2% for ITS. The LSU

dataset consisted of 21 terminals and 1208 characters. The tree topologies inferred using the LSU dataset from the nuclear DNA showed that the genus *Strigea* is paraphyletic because the genus was subdivided into two major clades. The first major clade was formed by two sequences identified as *Strigea robusta*

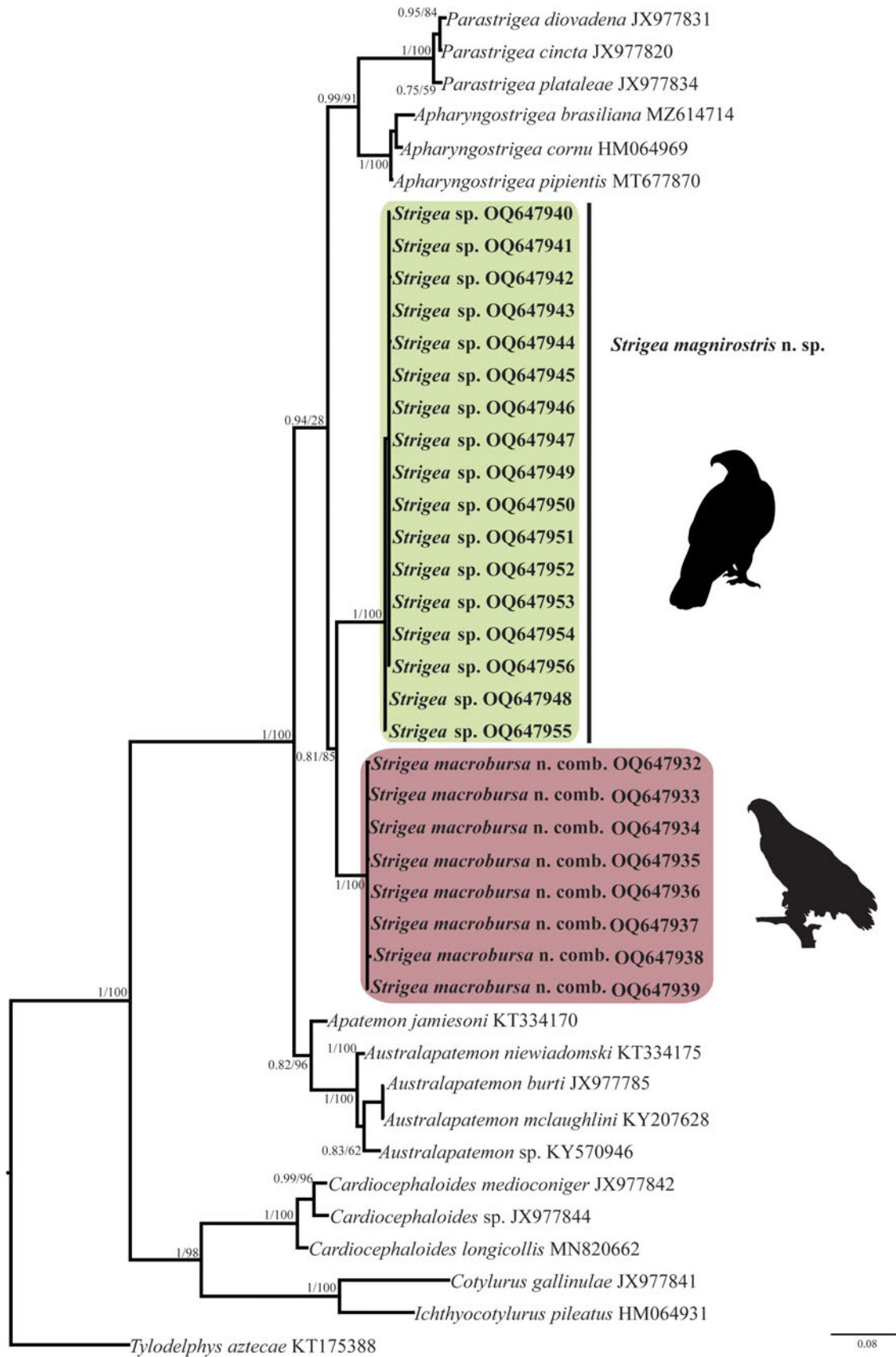


Fig. 2. Phylogenetic trees inferred with Maximum Likelihood (ML) and consensus Bayesian Inference (BI) with the internal transcribed spacers dataset. Numbers near internal nodes show maximum likelihood bootstrap percentage values and Bayesian posterior probabilities.

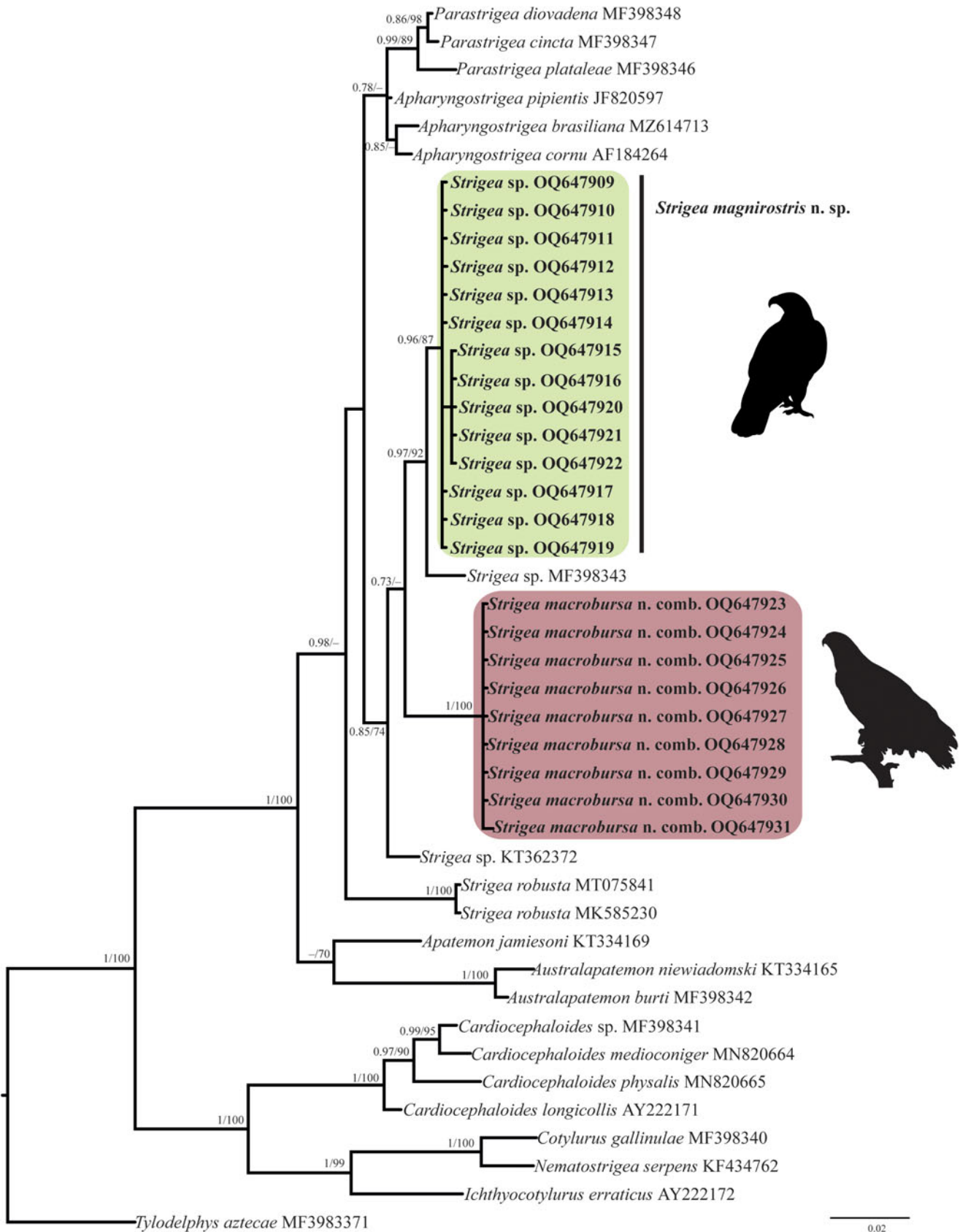


Fig. 3. Phylogenetics trees inferred with Maximum Likelihood (ML) and consensus Bayesian Inference (BI) with the large subunit dataset. Numbers near internal nodes show ML bootstrap percentage values and Bayesian posterior probabilities.

(MT075841 and MK585230) recovered from the marsh frog (*Pelophylax ridibundus*) and edible frog (*Pelophylax esculentus*), respectively, from Russia, and this clade was sister to a clade formed by species of the genera *Parastrigea* Szidat, 1928 and *Apharyngostrigea* Ciurea, 1927 (fig. 3). The second major clade was formed by four subclades. The first subclade contains an unidentified sequence of *Strigea* sp. (KT362372) from water frog (*Pelophylax* sp.) from France. The second subclade was formed by nine isolates of *P. macrobursa* from Mexico, which is a sister to the third subclade formed by a single sequence of an unidentified sample of *Strigea* sp. (MF398343) recovered from crested caracara (*Caracara cheriway*) from Presa La Angostura, Chiapas, Mexico. The fourth subclade was formed by 14 isolates of *Strigea* sp. recovered from the roadside hawk (*R. magnirostris*) and Cooper's hawk (*A. cooperii*) from six localities in Mexico (fig. 3). Finally, the intraspecific genetic divergence among 14 isolates of *Strigea* sp. was low, ranging from 0 to 0.10%, whereas that for nine isolates of *P. macrobursa* ranged from 0 to 0.08% for LSU.

Mitochondrial gene

The newly completed sequences from *cox 1* were aligned with other partial sequences downloaded from GenBank. The alignment included the first region of *cox 1* with 42 sequences and 374 characters. The phylogenetic analyses performed with ML and BI showed that the genus *Strigea* is monophyletic (fig. 4). The clade was subdivided into three subclades. The first subclade was formed by 16 isolates of an undescribed species of *Strigea* sp. from the Neotropical region of Mexico. The second subclade was formed by an isolate of an unidentified sequence of *Strigea* sp. (MF398319) from Presa La Angostura, Chiapas, Mexico. The third subclade was formed by seven isolates identified morphologically as *P. macrobursa*. All these relationships had high bootstrap values and Bayesian posterior probabilities (fig. 4). The intraspecific genetic divergence ranged from 0 to 1% among isolates of *Strigea* sp. and from 0 to 1.3% for *P. macrobursa* for *cox 1*.

In summary, the phylogenetic analyses performed with two nuclear markers and one mitochondrial molecular marker supported the monophyly of all new isolates of *Strigea* spp. from the Neotropical region (figs 2–4). The new ITS, LSU and *cox 1* sequences revealed that our specimens of *Strigea* sp. recovered from the roadside hawk (*R. magnirostris*) and Cooper's hawk (*A. cooperii*) from six localities in the Neotropical region of Mexico formed an independent lineage, which is recognized herein as a new species and is described next as *Strigea magnirostris* n. sp., representing the first species to Mexico and the 22nd to the Americas. In addition, the specimens identified as *P. macrobursa* collected from the intestine of the great black hawk (*B. urubitinga*) (type host) and common black hawk (*B. anthracinus*) formed a clade nested inside *Strigea*, and as a result, it should be transferred to *Strigea* to form *Strigea macrobursa* n. comb. (figs 2–4).

Morphological description

Family Strigeidae Railliet, 1919

Subfamily Strigeinae Railliet, 1919

Genus *Strigea* Abildgaard, 1790

Strigea magnirostris n. sp.

Type host: *R. magnirostris* (roadside hawk) (Accipitriformes: Accipitridae).

Other host: *A. cooperii* (Cooper's hawk) (Accipitriformes: Accipitridae).

Type locality: Tamiahua, Veracruz, Mexico (21°18'02" N, 97°26'56.2" W).

Other locality: Tres Vidas, Guerrero, Mexico (16°43'59.8" N, 99°42'48.9" W).

Site in host: Intestine.

Prevalence: eight of 11 (72%).

Type material: Holotype CNHE 11118; paratypes CNHE 11119; voucher CNHE 11120.

GenBank accession number: ITS, OQ647940–56; LSU, OQ647909–22; *cox 1*, OQ648135–50.

Etymology: The epithet of the species refers to the specific name of the type host.

Description (figs 5 and 6; table 2)

Description (based on 17 adult specimens) (figs 5 and 6): Body 3.03–4.43 mm (3.93 mm) in total length. Tegument spines on the surface of the forebody (fig. 6d). Forebody is longer than is wide, covered with tiny rounded spines, 562–872 (749) long by 400–690 (583) wide, representing 20% of body length (BL) (figs 5 and 6b–d). Hind-body long, strongly curved dorsally with tegument smooth, 2440–3591 (3176) long by 352–632 (492) wide, almost four times longer than the forebody, with a ratio of hind-body length to forebody length of 1: 3.3–5.3 (4.2). Oral sucker terminal, well developed, 77–109 (97) long by 80–115 (100) wide, with several papillae around it (fig. 6c). Ventral sucker well developed, larger than oral sucker, 150–240 (187) long by 124–188 (158) wide. Ratio of ventral sucker length to oral sucker length is 1: 1.45–2.42 (2.0). Pharynx 65–103 (80) long by 64–90 (72) wide. Ratio of pharynx length to oral sucker length is 0.84–1.10 (0.97). Pseudosuckers well developed with conspicuous folds in anterior section, 114–248 (185) long by 77–12 (101) wide (fig. 6b). Holdfast organ lobes can be projected beyond the anterior margin of the forebody, proteolytic gland at base of forebody, 182–225 (200) long by 83–119 (106) wide. Testes in tandem, bilobed, situated near posterior end of the body, anterior testis 272–476 (370) long by 261–496 (378) wide, posterior testis slightly larger than anterior testis at 346–497(420) long by 280–512 (400) wide. Seminal vesicle long, sinuous, posttesticular, slightly overlapping with posterior testis. Ovary reniform, pretesticular 139–190 (165) long by 126–214 (170) wide. Mehlis' gland and vitelline reservoir in the intertesticular region. Vitelline follicles of different sizes in both body segments; in the forebody, small follicles extend into the holdfast organ and lateral body wall from the posterior margin of the sucker ventral, while in the hind-body, large follicles are mostly concentrated in the neck (pre-ovarian region) ventrally to the seminal vesicle or copulatory bursa (fig. 5). Copulatory bursa large triangle-shaped broadening in posterior end, 247–531 (390) long by 468–784 (630) wide (figs 5 and 6e). Muscular ring (*Ringnapf*) well developed. Genital cone large and well delimited from body parenchyma, 193–361 (280) long by 380–637 (512) wide, ejaculatory duct and uterus join at base of genital cone, forming hermaphroditic duct. Uterus with large and numerous eggs (20–50) (35), oval, 71–105 long by 40–65 (52) wide. Ratio of genital cone length to egg length is 1: 1.95–3.88 (2.9). Excretory pore terminal.

Remarks

Currently, 21 species of the genus *Strigea* have been described in the Americas that parasitize strigiform, ciconiiform, falconiform, caprimulgiform, passeriform, gruiform, trogoniform and anseriform birds. Of the 21 described species, only five species (*S. falconis brasiliensis*, *S. elegans*, *S. microbursa*, *S. magniova* and *S. arcuata*) share morphological characteristics with *S. magnirostris*

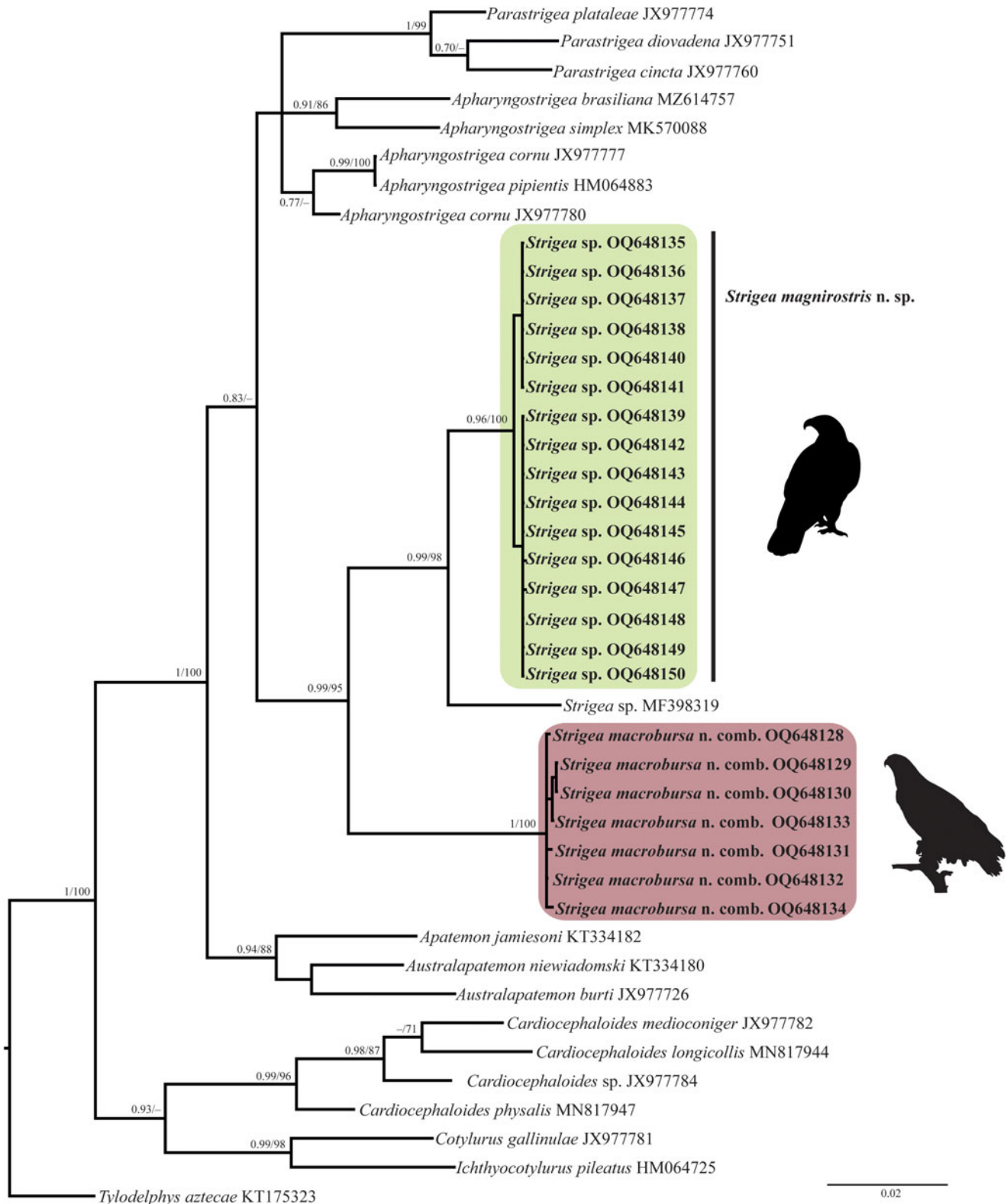


Fig. 4. Phylogenetics trees inferred with Maximum Likelihood (ML) and consensus Bayesian Inference (BI) with the *cox 1* dataset. Numbers near internal nodes show ML bootstrap percentage values and Bayesian posterior probabilities.

n. sp., such as body shape, presence of a neck region in the hind-body and distribution of vitelline follicles in the forebody, which are scarce and extend into the lobes from the holdfast organ (Chandler & Rausch, 1947; Dubois, 1968, 1988; Pearson &

Dubois, 1985; Lunaschi & Drago, 2006, 2009). The new species most closely resembles *S. arcuata*, *S. microbursa* and *S. elegans* by having pseudosuckers that are well developed in the forebody. However, *S. arcuata* can be distinguished from *S. magnirostris*

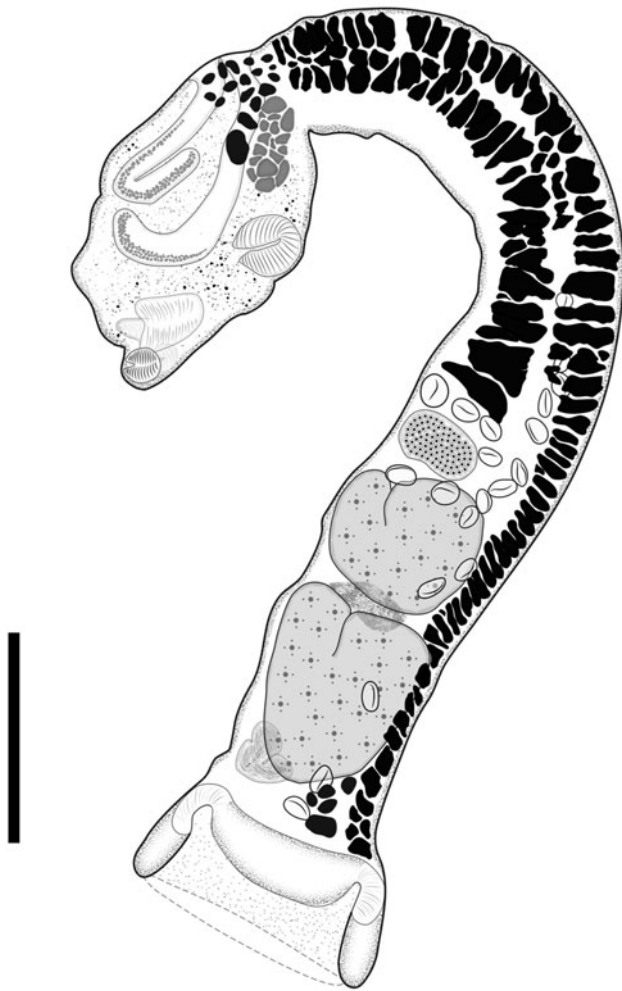


Fig. 5. Adult of *Strigea magnirostris* n. sp. from *Rupornis magnirostris*; whole worm, holotype, lateral view. Scale bars = 500 μ m.

n. sp. by having a smaller genital cone included in a circular muscular formation (125×145 vs. $193\text{--}361 \times 296\text{--}637$ in *S. magnirostris*). In addition, *S. arcuata* possesses lower limits for the following characteristics: pseudosuckers (105×80 vs. $118\text{--}248 \times 64\text{--}125$ in *S. magnirostris*); hind-body width (180 vs. $352\text{--}632$); anterior testes (255×185 vs. $272\text{--}476 \times 261\text{--}496$); and posterior testes (340×260 vs. $300\text{--}497 \times 280\text{--}512$). The species *S. microbursa* can be distinguished from *S. magnirostris* n. sp. by having a smaller genital cone ($100\text{--}180 \times 80\text{--}140$ vs. $193\text{--}361 \times 296\text{--}637$). In addition, *S. microbursa* possesses lower limits for the following characteristics: pseudosuckers ($85\text{--}95 \times 90\text{--}95$ vs. $118\text{--}248 \times 64\text{--}125$ in *S. magnirostris*); forebody width ($230\text{--}300$ vs. $400\text{--}690$); ovary length ($55\text{--}140$ vs. $139\text{--}190$); and ovary width ($80\text{--}106$ vs. $126\text{--}214$). Finally, *S. elegans* can be distinguished from *S. magnirostris* n. sp. due to its smaller BL ($1550\text{--}2450$ vs. $3030\text{--}4437$), smaller copulatory bursa (350 diam. vs. $247\text{--}531 \times 468\text{--}784$) and larger eggs ($115\text{--}220$ vs. $71\text{--}105$) (see table 2).

Morphological redescription

Strigea macrobursa n. comb.

Syn. *Parastrigea macrobursa* Drago and Lunaschi, 2011

Host: *B. urubitinga* (great black hawk) (Accipitriformes: Accipitridae).

Other host: *B. anthracinus* (common black hawk) (Accipitriformes: Accipitridae)

Locality: Isla Aguada, Campeche, Mexico ($18^{\circ}48'22.92''$ N, $91^{\circ}28'03.68''$ W).

Other localities: Tecolutla, Veracruz, Mexico ($20^{\circ}33'49.8''$ N, $97^{\circ}05'57.7''$ W).

Site in host: Intestine.

Prevalence: 3 of 6 (50%).

Voucher specimens: CNHE 11121, 11122.

GenBank accession number: ITS OQ647932–39; LSU OQ647923–31; *cox 1* OQ648128–34.

Description (figs 7 and 8; table 3)

Description (based on 26 adult specimens) (figs 7 and 8): Body $957\text{--}2.88$ mm (1920 mm) in total length. Forebody tulip-shaped, $344\text{--}775$ (560) long by $238\text{--}562$ (400) wide (fig. 7b). Tegument spines on the surface of the forebody (fig. 8d). Hind-body slightly plump with tegument smooth, two to three times longer than the forebody at $609\text{--}2184$ (1400) long by $256\text{--}759$ (508) wide, with some specimens having a neck region (nine individuals) and some specimens lacking a neck region (17 individuals) (fig. 7a, c). Ratio of BL to forebody length is 1: 2.5–4.1 (1: 3.3). Ratio of hind-body length to forebody length is 1: 1.5–3.1 (1: 2.3). Oral sucker subterminal, well developed, $64\text{--}95$ (80) long by $57\text{--}86$ (71) wide (fig. 8c). Ventral sucker oval, $74\text{--}106$ (90) long by $55\text{--}98$ (76) wide. Prepharynx absent, pharynx $33\text{--}66$ (52) long by $31\text{--}59$ (47) wide. Holdfast organ lobes reaching anterior end (fig. 8b, c), proteolytic gland at base of forebody 75 long by 43 wide. Testes in tandem, large, not lobed, anterior testis oval $95\text{--}281$ (190) long by $132\text{--}449$ (290) wide, posterior testis slightly larger than anterior testis at $137\text{--}392$ (260) long by $155\text{--}474$ (314) wide. Seminal vesicle long, posttesticular. Ovary oval, pre-testicular or slightly overlapping anterior testis, $52\text{--}188$ (120) long by $72\text{--}193$ (130) wide. Laure's canal, opening dorsally between ovary and anterior testis. Mehlis' gland and vitelline reservoir in the intertesticular region. Vitelline follicles similar in size in both body segments; in the forebody, they are in the dorsal lip of the holdfast organ forming two symmetrical masses situated between the ventral sucker and intersegmental constriction; in the hind-body, the vitelline follicles are concentrated in the pre-ovarian region, extending ventrally to the posterior testis or copulatory bursa (fig. 7a–c). Copulatory bursa large, delimited by pronounced constriction, occupying 30%–45% (40%) of hind-body length, $163\text{--}681$ (422) long by $246\text{--}616$ (430) wide (fig. 8e). Muscular ring (*Ringnapf*) absent. Genital cone well delimited from body parenchyma, $89\text{--}255$ (170) long by $137\text{--}230$ (180), ejaculatory duct and uterus join at base of genital cone forming hermaphroditic duct. Uterus with large and numerous eggs $3\text{--}50$ (26) that are $72\text{--}117$ (95) long by $45\text{--}67$ (56) wide. Ratio of BL to egg length is 1: 10–28 (1: 19). Genital atrium very deep, genital pore terminal. Excretory pore dorso-subterminal at the level of the copulatory bursa (see table 3).

Remarks

This species was originally described as *P. macrobursa* by Drago & Lunaschi (2011) from the great black hawk (*B. urubitinga*) from Argentina. The specimens collected in the present study are similar to those of the original description by Drago & Lunaschi (2011). For instance, a forebody tulip-shaped and vitelline follicles distributed in two lateral expansions and a large well-delimited copulatory bursa, with a well-delimited genital cone and deep genital atrium. However, the newly collected specimens from the great black hawk (type host) and common black hawk in

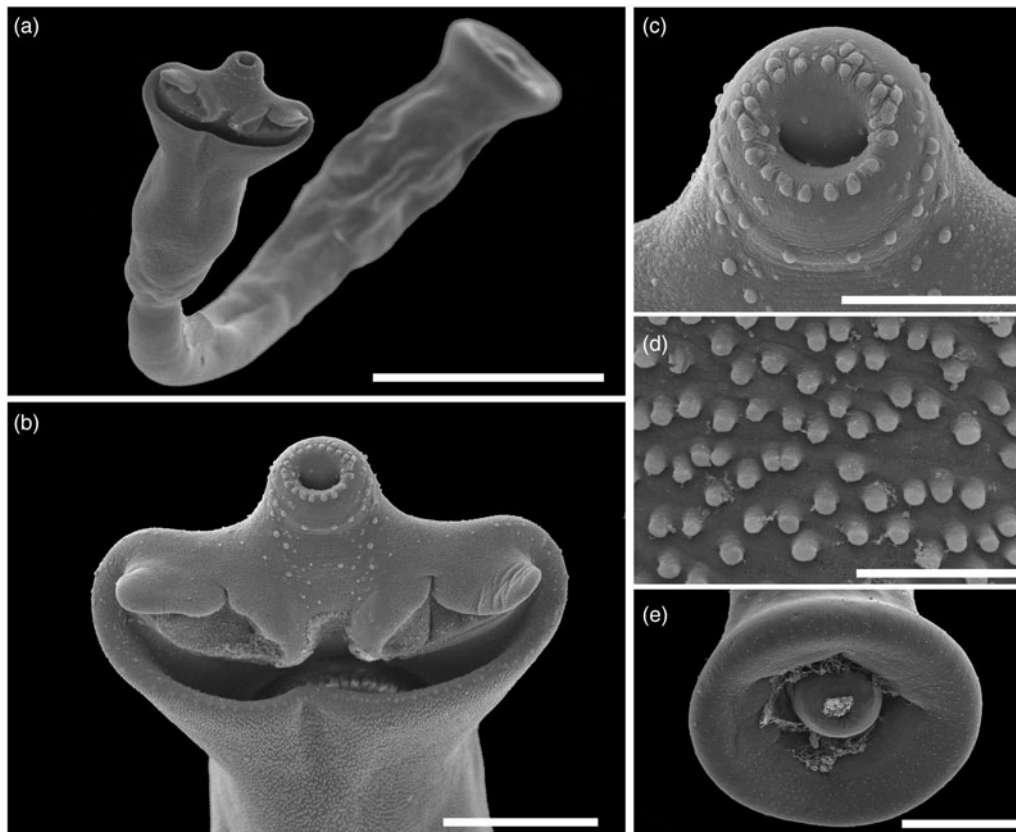


Fig. 6. Scanning electron micrographs of *Strigea magnirostris* n. sp. from *Rupornis magnirostris*. (a) Whole worm, ventral view; (b) forebody, ventral view showing pseudo-suckers; (c) oral sucker with papillae; (d) tegumental spines, ventral view of the forebody; (e) copulatory bursa showing cone genital. Scale bars: (a) 400 μ m; (b, e) 100 μ m; (c) 50 μ m; (d) 10 μ m.

three localities from the Neotropical region of Mexico showed some level of morphological intraspecific variation. For example, some of our specimens exhibit a neck in the hind-body, whereas other specimens do not. In addition, our specimens have tegumental spines that gradually diminish in size and number from the anterior to posterior region. However, apparently the presence or absence of spines could be related to the development of the worms. A similar pattern has been observed in specimens of two species, *S. falconis brasiliiana* and *S. elliptica*, from the Neotropical region (Lunaschi & Drago, 2006, 2009). Finally, our specimens possess higher limits than original description for the following characteristics: hind-body length (609–2184 vs. 754–1451); ovary length (52–188 vs. 69–131); anterior testes width (132–449 vs. 188–262); and posterior testes width (155–474 vs. 193–304) (see table 3).

Discussion

The taxonomic history and species composition of the family Strigeidae have been complex and unsettled. Recent molecular evidence suggests that the family is paraphyletic. However, the genera *Apharyngostrigea*, *Parastrigea* and *Strigea* share a common ancestor (Blasco-Costa *et al.*, 2016; Blasco-Costa & Locke, 2017; Hernández-Mena *et al.*, 2017; Locke *et al.*, 2021; López-Jiménez *et al.*, 2022). The genetic library of some strigeid species of the genera *Apharyngostrigea*, *Parastrigea* and *Strigea* has recently increased and provides a large opportunity to clarify the taxonomy and species composition of these three genera

(Blasco-Costa *et al.*, 2016; Hernández-Mena *et al.*, 2017; Locke *et al.*, 2021; López-Jiménez *et al.*, 2022). In the current study, we combined morphological and molecular characteristics to describe a new species, *S. magnirostris* n. sp. that represents the first species in the Neotropical region of Mexico and the 22nd in the Americas. Morphologically, the new species is distinguished from other congeneric species from the Americas by having an oral sucker with several papillae around it, well-developed pseudosuckers, a tegument covered with tiny spines, a larger cone genital and a larger copulatory bursa. In addition, the phylogenetic trees established with three molecular markers supported that the isolates identified morphologically as *P. macrobursa* from *B. urubitinga* (type host) and *B. anthracinus* collected from three localities in Mexico are not closely related to other members of the genus *Parastrigea* because they were nested inside *Strigea*. Therefore, we transferred it to *Strigea* to form *S. macrobursa* n. comb., expanding its geographical distribution from Mexico to Argentina (Drago & Lunaschi, 2011), representing the first record in Mexico. Interestingly, our phylogenies established that *S. magnirostris* n. sp., *S. macrobursa* n. comb. and *Strigea* sp. were associated with accipitriform and falconiform birds from the Neotropical region on a clade, suggesting that at least two clades could be formed, one represented by the 22 described species from the Neotropical region and the second represented by the six species from the Nearctic region in the Americas. However, this hypothesis should be tested with more species from other biogeographical regions and primarily adult specimens because the sequences from the LSU available in

Table 2. Comparative measurements of *Strigea magnirostris* n. sp. and related species.

	<i>Strigea magnirostris</i> n. sp.	<i>Strigea arcuata</i>	<i>Strigea microbursa</i>		<i>Strigea elegans</i>	<i>Strigea magniova</i>	<i>Strigea falconis</i> <i>brasiliiana</i>	
Source	Present study	Dubois (1988)	Pearson & Dubois (1985)	Lunaschi & Drago, (2009)	Chandler & Rausch (1947)	Dubois (1988)	Dubois (1968)	Lunaschi & Drago (2006)
Locality	Mexico	Paraguay	Indonesia	Argentina	United States	Paraguay	Brazil, Cuba	Argentina
Host	<i>Rupornis magnirostris</i> <i>Accipiter cooperii</i>	<i>Accipiter erythronemius</i> <i>Parabuteo unicinctus</i>	<i>Spilornis cheela</i>	<i>Buteogallus meridionalis</i>	<i>Bubo virginianus</i>	<i>R. magnirostris</i>	Accipitridae Falconidae	<i>R. magnirostris</i>
Body length	3030–4437	3700	1400–3600	1266–3021	1550–2450	1320	up to 2500	1305–1392
Forebody (Fo)	562–872 × 400–690	900 × 600	420–600 × 230–300	832–1083 × 328–551	560–1050 × 420–560	320–340 × 230–240	380–590 × 420–700	319–415 × 314–367
Hind-body (Hi)	2440–3591 × 352–632	2800 × 180	900–1200 × 170–220	1083–2102 × 232–435	980–1800 × 320–500	850–1000 × 160–260	1110–1830 × 340–580	890–1073 × 362–435
Pseudo-suckers	118–248 × 64–125	105 × 80	85–95 × 90–95	–	–	–	–	–
Oral sucker	72–109 × 80–115	110 × 105	68–117 × 70–127	69–107 × 74–117	110 × 130	48–68 × 48–57	100–125 × 85–115	76 × 55
Ventral sucker	142–240 × 119–188	200 × 135	65–122 × 73–138	107–143 × 116–143	198 × 220	55–63 × 70–78	160–235 × 140–200	152–162 × 71–105
Proteolytic gland	157–225 × 66–119	185 × 115	–	143–193 × 126–152	150 × 180	–	105–130 × 120–190	–
Pharynx	65–103 × 64–90	95 × 90	57–132 × 52–150	62–83 × 52–64	–	30 × 28	73–95 × 70–95	74 × 48
Ovary	139–190 × 126–214	140 × 170	55–140 × 80–106	105–138 × 88–217	150 × 165	52–65 × 60–80	110–200 × 175–300	59–68 × 101–107
Anterior testis	272–476 × 261–496	255 × 185	110–150 × 130–190	143–280 × 131–343	400 × 425	120–160 × 130–195	235–360 × 235–410	169–227 × 174–190
Posterior testis	300–497 × 280–512	340 × 260	110–190 × 150–190	179–241 × 157–314	400 × 430	130–150 × 140–220	275–370 × 235–420	197–217 × 179–241
Copulatory bursa	247–531 × 468–784	–	–	104–420 × 102–381	350 diameter	–	–	183–241 × 215–226
Genital cone	193–361 × 296–637	125 × 145	100–180 × 80–140	–	–	95–115 × 98–105	240–350 × 220–310	128–167 × 129–143
<i>n</i> eggs	8–50	32 ^a	1–3	1–3	1–8	3–7	1–3	3–5
Eggs	71–105 × 40–65	84–96 × 55–63	100–105 × 50–57	83–129 × 52–98	115–220 × 65–73	105–115 × 52–60	67–91 × 42–55	82–88 × 48–52
Ratio Hi/Fo length	3.2–5.3	3.1 ^a	2.0–2.1 ^a	1.2–2.3	1.4–2.3	2.6–2.9 ^a	1.8–3.6	2.1–3.4
Ratio Vs/Os	1.3–1.8	1.2 ^a	1 ^a	1.2–1.5 ^a	1.6 ^a	1.3–1.4 ^a	1.6–1.7 ^b	1.9
Ratio Ph/Os	0.7–0.9	0.8 ^a	0.7–1.1 ^a	0.7–1	–	0.4–0.5 ^a	0.8 ^b	0.9 ^b
Ratio Hi/Gc	9.2–15.1	22.4 ^a	6.6–9 ^a	–	–	8.6–8.9 ^a	4.6–5.2 ^b	6.4–7 ^b
Ratio Gc/E	1.9–3.8	1.4	1–1.7 ^a	–	–	0.9–1 ^a	3–5 ^b	1.5–2 ^b

Gc/eggs, genital cone length/egg length; Hi/Fo, hind-body length/forebody length; Hi/Gc, hind-body length/genital cone length; Ph/Os, pharynx width/oral sucker width; Vs/Os, suckers width ratio.

^aCalculated from original descriptions.^bCalculated from original descriptions by Drago *et al.* (2014).

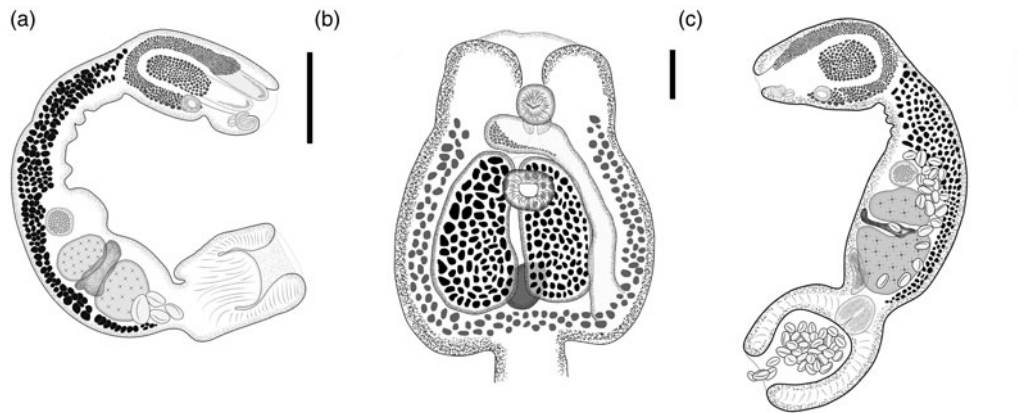


Fig. 7. Adult of *Strigea macrobursa* n. comb. from *Buteogallus urubitinga*. (a) Whole worm; (b) forebody, ventral view; (c) whole worm. Scale bars: (a) 300 μ m; (b) 100 μ m; (c) 250 μ m.

GenBank are from larval forms of *Strigea* spp. (KT362372, MT075841 and MK585230) (Patrelle *et al.*, 2015; Svinin *et al.*, 2020).

Heneberg *et al.* (2018) performed one of the most comprehensive taxonomic reviews of strigeids that included samples of the genera *Strigea*, *Parastrigea*, *Apharyngostrigea*, *Cotylurus* Szidat, 1928 and *Apatemon* Szidat, 1928 from Central Europe. These authors sequenced the small subunit and the ITS2 from nuclear

ribosomal DNA and the second region of the barcode from *cox 1* and nicotinamide adenine dinucleotide dehydrogenase subunit 1 from mitochondrial DNA. However, these authors could not compare their sequences with other sequences of strigeids previously analysed by Hernández-Mena *et al.* (2014, 2017) and Blasco-Costa *et al.* (2016) because these authors sequenced the ITS (ITS1-5.8S rDNA- ITS2), the domains D1–D3 of the LSU from nuclear DNA and the *cox 1* barcode, the first region from

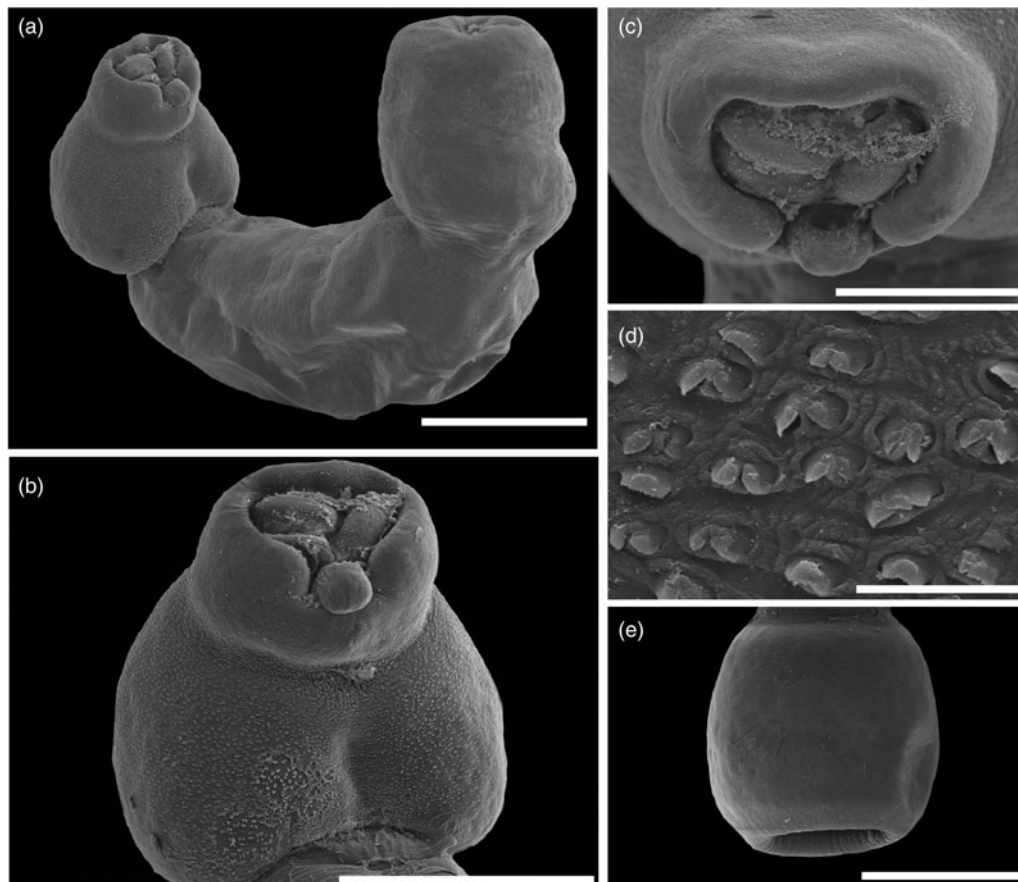


Fig. 8. Scanning electron micrographs of *Strigea macrobursa* n. comb. from *Buteogallus urubitinga*. (a) Whole worm, ventral view; (b) forebody, ventral view; (c) oral sucker; (d) tegumental spines; (e) copulatory bursa. Scale bars: (a) 500 μ m; (b, e) 400 μ m; (c) 200 μ m; (d) 10 μ m.

Table 3. Comparative measurements of adults *Strigea macrobursa* Drago & Lunaschi, 2011 recorded in the Americas.

	<i>Strigea macrobursa</i> n. comb.	<i>Strigea macrobursa</i> (syn. <i>Parastrigea macrobursa</i>)
Source	Present study	Drago & Lunaschi (2011)
Locality	Mexico	Argentina
Host	<i>Buteogallus urubitinga</i> <i>Buteogallus anthracinus</i>	<i>B. urubitinga</i>
Body length	957–2886	1189–2117
Forebody (Fo)	344–775 × 238–562	435–783 × 348–638
Hind-body (Hi)	609–2184 × 256–759	754–1451 × 391–658
Neck	130–576 × 94–291	–
Oral sucker	64–95 × 57–86	76–87 × 64–99
Ventral sucker	74–106 × 55–98	82–107 × 60–150
Proteolytic gland	75 × 53	64–83 × 60–76
Pharynx	34–66 × 31–59	44–60 × 39–60
Ovary	52–188 × 72–193	69–131 × 109–190
Anterior testis	95–281 × 132–449	97–155 × 188–262
Posterior testis	137–392 × 155–474	102–213 × 193–304
Copulatory bursa	163–681 × 246–616	290–648 × 280–532
Genital cone	89–255 × 137–230	117–179 × 107–176
<i>n</i> eggs	3–50	3–45
Eggs	72–117 × 45–67	92–143 × 57–77
Ratio Hi/Fo	1.5–3.1	1.7–3.1
Ratio BL/Fo	2.5–4.1	2.7–4.1
Ratio BL/E	10–28	10–20

BL/Fo, body length/forebody length; BL/E, body length/eggs length; Hi/Fo, hind-body length/forebody length.

the mitochondrial DNA. These three molecular markers have proven very useful for delineating species and inferring phylogenetic relationships at the genus level within Strigeidae. Herein, we compared the sequences of Heneberg *et al.* (2018) with other sequences available in GenBank and with the newly generated sequences. We generated two new alignments. The first includes 60 sequences of ITS2 with 320 bp, representing 30% (1042 bp) of our original dataset that contains ITS1-5.8S rDNA-ITS2. Our phylogenetic trees established with ITS2 were similar to the tree inferred by Heneberg *et al.* (2018), including the polyphyly of *Strigea*, with weak bootstrap support and posterior probabilities. In addition, the isolates of the new species *S. magnirostris* n. sp. plus *S. macrobursa* formed a clade together with *S. falconis* (MF628087) (see online supplementary fig. S1). The second alignment contained 46 sequences of *cox 1* (including the newly generated sequences in the current study) with 297 bp of the second region of the barcode. The phylogenetic trees placed all the species of *Strigea*, including the new species *S. magnirostris* n. sp. and *S. macrobursa* in a clade. However, the species *Parastrigea flexilis* Dubois, 1934 (MF628065) was nested inside *Strigea*, suggesting that *P. flexilis* should be transferred to *Strigea* (see online supplementary fig. S2). To clarify the taxonomy of the genera *Strigea*, *Parastrigea* and *Apharyngostrigea*, it is necessary to review the taxonomy of the species that share diagnostic characteristics among the three genera. For instance, *Parastrigea* is characterized by the distribution of vitellaria (two symmetrical masses on the forebody), which are present in *S. falconis*, *S. strigis* (Schrank,

1788) Abildgaard, 1790, *S. robusta* (Szidat, 1928) Heneberg and Sitko, 2018, *Apharyngostrigea brasiliiana* Szidat, 1928 (Dubois, 1964) and *S. macrobursa* n. comb., (Dubois, 1968; Heneberg *et al.*, 2018; López-Jiménez *et al.*, 2022).

In summary our phylogenetic trees established with ITS and *cox 1* supported the monophyly of *Strigea*. However, the LSU tree showed that *Strigea* is paraphyly because two sequences of larval forms identified as *S. robusta* (MT075841 and MK585230) were nested inside other clades. In addition, the genetic divergence among the species of the first clade of *Strigea*, *S. magnirostris* n. sp., *S. macrobursa* and two isolates of *Strigea* sp. (MF398343 and KT362372), ranged from 0.6% to 1.6% and from 2.4% to 2.8% with respect to *S. robusta*. These high ranges of divergence are similar between *Strigea* and *Apharyngostrigea*, which ranged from 1.9% to 2.2% for the LSU marker. The phylogenetic analyses established with the LSU, in combination with the high genetic divergence, of the two sequences of larval forms identified as *S. robusta* suggests that they do not belong to *Strigea*. However, the ITS2 tree (see online supplementary file S1) placed five isolates of *S. robusta* of adult and larval forms (MF537205, MT075803, MK295777, MF537208 and MF628100) from Germany, Russia and Poland in a single clade that is a sister to the type species.

In the current study, we described a new species of *Strigea*, collected from the intestines of two hawk species (*R. magnirostris* and *A. cooperii*) which is named *S. magnirostris* n. sp. In addition, the species *P. macrobursa* was transferred to *Strigea* to form

S. macrobursa n. comb. To clarify the taxonomy of the genus *Strigea*, it is necessary to sequence more species (including the type species, *S. strigis*) from diverse biogeographical regions with the ITS (ITS1-5.8S rDNA- ITS2), the D1-D3 domains from the LSU and the first region from the *cox 1* gene. Finally, the current integrative study represents a continuation of our effort in describing and understanding the biodiversity of strigeids in the Neotropical region.

Supplementary material. To view supplementary material for this article, please visit <https://doi.org/10.1017/S0022149X23000196>.

Acknowledgements. We are grateful to Laura Marquez and Nelly López for their help during the sequencing of the DNA fragments. We also thank Berenit Mendoza Garfias for her help in obtaining the scanning electron microphotographs.

Financial support. ALJ and MTGG thank the support of the Programa de Posgrado en Ciencias Biológicas, UNAM and CONACYT (ALJ. CVU. No. 706119; MTGG. CVU. No. 956064) for granting a scholarship to complete her PhD program and his Master program, respectively. LAG thanks the Coordinación de la Investigación Científica and Dirección General de Asuntos de Personal Académico (DGAPA-UNAM) Mexico for the Postdoctoral Fellowship granted. This research was supported by the Programa de Apoyo a Proyectos de Investigación e Innovación Tecnológica (PAPIIT-UNAM) IN201122.

Competing interests. None.

Author contributions. ALJ and MGJ conceived and designed the study. ALJ and MTGG conducted data gathering. ALJ, LAG and MTGG performed statistical analyses. ALJ, LAG and MGJ wrote and edited the article. ALJ, MTTG, LAG and MGJ collected the samples. ALJ performed the methodology.

Ethical standards. The sampling in this work complies with the current laws and animal ethics regulations of Mexico.

References

- American Ornithologist' Union** (1998) *Checklist of North American birds*. 7th edn. 829 pp. Washington, DC, American Ornithologist' Union.
- Blasco-Costa I and Locke SA** (2017) Life history, systematics and evolution of the Diplostomoidea Poirier, 1886: progress, promises and challenges emerging from molecular studies. pp. 167–225 in Rollinson D and Stothard JR (Eds), *Advances in parasitology*. USA, Academic Press.
- Blasco-Costa I, Poulin R and Presswell B** (2016) Species of *Apatemon* Szidat, 1928 and *Australapatemon* Sudarikov, 1959 (Trematoda: Strigeidae) from New Zealand: linking and characterising life cycle stages with morphology and molecules. *Parasitology Research* **115**(1), 271–289.
- Bowles J and McManus DP** (1993) Rapid discrimination of *Echinococcus* species and strains using a PCR-based method. *Molecular and Biochemical Parasitology* **57**(2), 231–239.
- Bowles J, Blair D and McManus DP** (1992) Genetic variants within the genus *Echinococcus* identified by mitochondrial DNA sequencing. *Molecular and Biochemical Parasitology* **54**(2), 165–173.
- Bowles J, Blair D and McManus DP** (1995) A molecular phylogeny of the human schistosomes. *Molecular Phylogenetics and Evolution* **4**(2), 103–109.
- Chandler AC and Rausch R** (1947) A study of strigeids from owls in North Central United States. *Transactions of the American Microscopical Society* **66**(3), 283–292.
- Drago F and Lunaschi L** (2011) A new species of *Parastrigea* (Digenea, Strigeidae) endoparasite of *Buteogallus urubitinga* (Aves, Accipitridae) from Argentina. *Helminthologia* **48**(4), 256–261.
- Drago F, Lunaschi L and Draghi R** (2014) Digenean fauna in raptors from northeastern Argentina, with the description of a new species of *Strigea* (Digenea: Strigeidae). *Zootaxa* **3785**(1), 258–270.
- Dubois G** (1968) Synopsis of the Strigeidae and of the Diplostomidae (Trematoda). *Memories de la Société Neuchâteloise des Sciences Naturelles* **10**(1), 1–258.
- Dubois G** (1988) Quelques Strigeoidea (Trematoda) récoltés au Paraguay par les expéditions du Muséum d'Histoire naturelle de Genève, au cours des années 1979, 1982 et 1985 [Some Strigeoidea (Trematoda) collected in Paraguay by expeditions from the Natural History Museum of Geneva, during the years 1979, 1982 and 1985]. *Revue Suisse de Zoologie* **95**(2), 521–532. [In French.]
- Dubois G and Beverley-Burton M** (1971) Quelques Strigeata (Trematoda) d'Oiseaux de Rhodésie et de Zambie [Some Strigeata (Trematoda) from Rhodesian and Zambian birds]. *Bulletin de la Société Neuchâteloise des Sciences Naturelles* **94**(1), 5–19. [In French.]
- García-Varela M and Nadler SA** (2005) Phylogenetic relationships of Palaeacanthocephala (Acanthocephala) inferred from SSU and LSU rDNA gene sequences. *Journal of Parasitology* **91**(6), 1401–1409.
- Heneberg P, Sitko J, Teš'inský M, Rząd I and Bizos J** (2018) Central European Strigeidae Railliet, 1919 (Trematoda: Strigeida): molecular and comparative morphological analysis suggests the reclassification of *Parastrigea robusta* Szidat, 1928 into *Strigea* Abildgaard, 1790. *Parasitology International* **67**(6), 688–701.
- Hernández-Mena DI, García-Prieto L and García-Varela M** (2014) Morphological and molecular differentiation of *Parastrigea* (Trematoda: Strigeidae) from Mexico, with the description of a new species. *Parasitology International* **63**(2), 315–323.
- Hernández-Mena DI, García-Varela M and Pérez-Ponce de León G** (2017) Filling the gaps in the classification of the Digenea Carus, 1863: systematic position of the Proterodiplostomidae Dubois, 1936 within the superfamily Diplostomoidea Poirier, 1886, inferred from nuclear and mitochondrial DNA sequences. *Systematic Parasitology* **94**(8), 833–848.
- Howell SNG and Webb S** (1995) *A guide to the birds of Mexico and Northern Central America*. 851 pp. New York, Oxford University Press.
- Locke SA, Drago FB, López-Hernández D, et al.** (2021) Intercontinental distributions, phylogenetic position and life cycles of species of *Apharyngostrigea* (Digenea, Diplostomoidea) illuminated with morphological, experimental, molecular and genomic data. *International Journal for Parasitology* **51**(8), 667–683.
- López-Jiménez A, Hernández-Mena DI, Solórzano-García B and García-Varela M** (2021) Exploring the genetic structure of *Parastrigea diovadena* Dubois and Macko, 1972 (Digenea: Strigeidae), an endoparasite of the white ibis, *Eudocimus albus*, from the Neotropical region of Mexico. *Parasitology Research* **120**(6), 2065–2075.
- López-Jiménez A, González-García MT and García-Varela M** (2022) Molecular and morphological evidence suggests the reallocation from *Parastrigea brasili-ana* (Szidat, 1928) Dubois, 1964 to *Apharyngostrigea* Ciurea, 1927 (Digenea: Strigeidae), a parasite of boat-billed heron (*Cochlearius cochlearius*) from the Neotropical region. *Parasitology International* **86**(1), 102468.
- Lunaschi L and Drago F** (2006) Strigeid parasites of the roadside hawk, *Buteo magnirostris* (Aves: Falconiformes), from Argentina. *Zootaxa* **1106**(1), 25–33.
- Lunaschi L and Drago F** (2009) Species of *Strigea* (Digenea: Strigeidae), parasites of the savanna hawk *Buteogallus meridionalis* (Aves: Accipitridae) from Argentina, with the description of a new species. *Folia Parasitologica* **56**(4), 268–274.
- Lunaschi L and Drago F** (2012) Digenean parasites of *Cariama cristata* (Aves, Gruiformes) from Formosa Province, Argentina, with the description of a new species of the genus *Strigea*. *Acta Parasitologica* **57**(1), 26–33.
- Lunaschi L and Drago F** (2013) Digenean parasites of the great antshrike, *Taraba major* (Aves: Thamnophilidae), from Argentina, with a description of a new species of the genus *Strigea* (Strigeidae). *Folia Parasitologica* **60**(4), 331–338.
- Miller MA, Pfeiffer W and Schwartz T** (2010) Creating the CIPRES science gateway for inference of large phylogenetic trees. pp. 1–8. In *Gateway Computing Environments Workshop*, 14 November 2010, New Orleans, LA, USA. Piscataway, NJ, Institute of Electrical and Electronics Engineers.
- Nadler SA, Hoberg EP, Hudspeth DSS and Rickard LG** (2000) Relationships of *Nematodirus* species and *Nematodirus battus* isolates (Nematoda: Trichostrongyloidea) based on nuclear ribosomal DNA sequences. *Journal of Parasitology* **86**(3), 588–601.

- Niewiadomska K** (2002) Family strigeidae. pp. 231–260. In Gibson DI, Jones A and Bray RA (Eds) *Keys to the Trematoda*. London, Publishing and the Natural History Museum.
- Odening K** (1967) Die Lebenszyklen von *Strigea falconispalumbi* (Viborg), *S. strigis* (Schrank) und *S. sphaerula* (Rudolphi) (Trematoda, Strigeida) im Raum Berlin [The life cycles of *Strigea falconispalumbi* (Viborg), *S. strigis* (Schrank) and *S. sphaerula* (Rudolphi) (Trematoda, Strigeida) in the Berlin area]. *Zoologische Jahrbücher Abteilung für Systematik* **94**(1), 1–67. [In German.]
- Patrelle C, Portier J, Jouet D, Delorme D and Ferte H** (2015) Prevalence and intensity of *alaria alata* (goetze, 1792) in water frogs and brown frogs in natural conditions. *Parasitology Research* **114**(12), 4405–4412.
- Pearson JC** (1959) Observations on the morphology and life cycle of *Strigea elegans* Chandler & Rausch, 1947 (Trematoda: Strigeidae). *Journal of Parasitology* **45**(2), 155–174.
- Pearson JC** (1972) A phylogeny of life-cycle patterns of the Digenea. pp. 153–189 in Dawes B (Ed.), *Advances in parasitology*. USA, Academic Press.
- Pearson JC and Dubois G** (1985) Strigeida d'Indonésie et de Malaisie, et quelques-uns d'Australie et de Tasmanie. I, Strigeoidea [Strigeida from Indonesia and Malaysia, and a few from Australia and Tasmania. I, Strigeoidea]. *Bulletin de la Société Neuchâteloise des Sciences Naturelles* **108**(1), 5–21. [In French.]
- Pérez-Ponce de León G, García-Prieto L and Mendoza-Gárfias B** (2007) Trematode parasites (Platyhelminthes) of wildlife vertebrates in Mexico. *Zootaxa* **1534**(1), 1–247.
- Posada D** (2008) jModelTest: phylogenetic model averaging. *Molecular Biology and Evolution* **25**(7), 1253–1256.
- Rambaut A** (2012) FigTree v1.4.2. Available at <http://tree.bio.ed.ac.uk/software/figtree/> (accessed 20 July 2021).
- Ronquist F, Teslenko M, Van Der Mark P, et al.** (2012) MrBayes 3.2: efficient Bayesian phylogenetic inference and model choice across a large model space. *Systematic Biology* **61**(3), 539–542.
- Silvestro D and Michalak I** (2012) raxmlGUI: a graphical front-end for RAxML. *Organisms Diversity & Evolution* **12**(4), 335–337.
- Sinsch U, Heneberg P, Těšínský M, Balczun C and Scheid P** (2019) Helminth endoparasites of the smooth newt *Lissotriton vulgaris*: linking morphological identification and molecular data. *Journal of Helminthology* **93**(3), 332–341.
- Svinin AO, Bashinskiy IV, Ermakov O and Litvinchuk S** (2023) Effects of minimum *Strigea robusta* (Digenea: Strigeidae) cercariae doses and localization of cysts on the anomaly P manifestation in *Pelophylax lessonae* (Anura: Ranidae) tadpoles. *Parasitology Research* **122**(3), 889–894.
- Svinin AO, Bashinskiy IV, Litvinchuk SN, et al.** (2020) *Strigea robusta* causes polydactyly and severe forms of Rostand's anomaly P in water frogs. *Parasites & Vectors* **13**(1), 381.
- Tamura K, Stecher G, Peterson D, Filipski A and Kumar S** (2013) MEGA6: molecular evolutionary genetics analysis version 6.0. *Molecular Biology and Evolution* **30**(12), 2725–2729.
- Thompson J, Gibson T, Plewniak F, Jeanmougin F and Higgins D** (1997) The CLUSTAL_X windows interface: flexible strategies for multiple sequence alignment aided by quality analysis tools. *Nucleic Acids Research* **25**(24), 4876–4882.
- Vidal-Martínez VM** (1995) *Processes structuring the helminth communities of native cichlid fishes from southern Mexico*. 164 pp. PhD thesis, Faculty of Science, University of Exeter, UK.